Spatial and temporal regulation of the endoproteolytic activity of the SPS-sensor–controlled Ssy5 signaling protease

António Martins[†], Andreas Ring[†], Deike J. Omnus, Stijn Heessen[‡], Thorsten Pfirrmann[§], and Per O. Ljungdahl*
Department of Molecular Biosciences, The Wenner-Gren Institute, Stockholm University, SE-106 91 Stockholm, Sweden

ABSTRACT **The *Saccharomyces cerevisiae* Ssy5 signaling protease is a core component of the plasma membrane (PM)–localized SPS (Ssy1-Ptr3-Ssy5) sensor. In response to extracellular amino acids, the SPS-sensor orchestrates the proteasomal degradation of the inhibitory Ssy5 prodomain. The unfettered catalytic (Cat)-domain cleaves latent transcription factors Stp1 and Stp2, freeing them from negative N-terminal regulatory domains. By studying the spatial and temporal constraints affecting the unfettered Cat-domain, we found that it can cleave substrates not associated with the PM; the Cat-domain efficiently cleaves Stp1 even when fused to the carboxy terminus of the endoplasmic reticulum (ER) membrane protein Shr3. The amino acid–induced cleavage of this synthetic membrane–anchored substrate occurs in a Δtether strain lacking ER–PM junctions. We report that the bulk of the Cat-domain is soluble, exhibits a disperse intracellular distribution, and is subject to ubiquitylation. Cat-domain ubiquitylation is dependent on Ptr3 and the integral PM casein kinase I (Yck1/2). Time-course experiments reveal that the non- and ubiquitylated forms of the Cat-domain are stable in cells grown in the absence of inducing amino acids. By contrast, amino acid induction significantly accelerates Cat-domain degradation. These findings provide novel insights into the SPS-sensing pathway and suggest that Cat-domain degradation is a requisite for resetting SPS-sensor signaling.**

Monitoring Editor
Thomas Sommer
Max Delbrück Center for Molecular Medicine

Received: Feb 11, 2019
Revised: Jul 19, 2019
Accepted: Aug 20, 2019

INTRODUCTION

The key event in protease-dependent signaling is an irreversible change of function of a physiological substrate (Turk, 2006). Once activated, a signaling protease cleaves its substrates, initiating the propagation of transducing signals. To be considered a physiological substrate, a protein has to physically interact with the active protease and then subsequently be cleaved (Turk *et al.*, 2012). Proteases are expressed as inactive zymogens and activation is usually achieved by limited proteolysis of an inhibitory prodomain, an event that typically occurs at the site where the protease exerts its biological function. This allows the spatial and temporal regulation of its activity, thereby helping to prevent unwanted proteolytic events (Khan and James, 1998). The proteolytic conversion of zymogens to active proteases is itself irreversible. To block unintentional proteolysis, cells have evolved elaborate mechanisms to maintain control of catalytic domains (Turk *et al.*, 2012). In the case of signaling proteases, cell must possess the ability to turn off the signal-induced protease when the inducing signals are no longer present, an obvious requisite for resetting and restoring the capacity of cells to sense and respond to inducing signals. Less obvious is how cells accomplish this.

The yeast *Saccharomyces cerevisiae* uses the Ssy1-Ptr3-Ssy5 (SPS) sensing pathway to respond to extracellular amino acids (Forsberg and Ljungdahl, 2001; Ljungdahl and Daignan-Fornier, 2012). Ssy1, the amino acid receptor, is an integral component of

This article was published online ahead of print in MBoC in Press (http://www.molbiolcell.org/cgi/doi/10.1091/mbc.E19-02-0096) on August 28, 2019.

†These authors contributed equally to this work.

The authors declare no competing financial interests.

A.M., A.R., D.J.O., S.H., T.P., and P.O.L. designed and analyzed experiments; A.M., A.R., and D.J.O. performed experiments; and A.M., A.R., and P.O.L. wrote the paper with contributions from D.J.O.

Present addresses: ‡Business Development, Branded Consumer Healthcare, Perrigo, 3062CE Rotterdam, The Netherlands; §Institute for Physiological Chemistry, Martin-Luther University Halle-Wittenberg, D-06114 Halle, Germany.

*Address correspondence to: Per O. Ljungdahl (per.ljungdahl@su.se).

Abbreviations used: β-gal, β-galactosidase; HA, hemagglutinin; MM, (2-{[({[(4-methoxy-6-methyl)-1,3,5-triazin-2-yl]-amino}carbonyl)amino]-sulfonyl}-benzoic acid; SD, synthetic minimal dextrose; SPS, Ssy1-Ptr3-Ssy5; YPD, yeast extract–peptone–dextrose; vc, vector control; WT, wild type.

the plasma membrane (PM) and a nontransporting member of the amino acid permease (AAP) protein family (Jørgensen *et al.*, 1998; Iraqui *et al.*, 1999; Klasson *et al.*, 1999; Wu *et al.*, 2006). Upon amino acid induction, in a strictly Ptr3-dependent manner, the SPS-sensor coordinates signaling events leading to the activation of the Ssy5 endoprotease (Andréasson and Ljungdahl, 2002; Abdel-Sater *et al.*, 2004; Andréasson, 2004; Andréasson *et al.*, 2006; Poulsen *et al.*, 2006). Ssy5 is a serine protease expressed as an inactive zymogen that during biogenesis is subject to an autocatalytic event that cleaves the regulatory N-terminal prodomain from the C-terminal catalytic-(Cat)-domain (Martins *et al.*, 2018). Importantly, the pro- and Cat-domains remain noncovalently associated. Thus, autolysis results in a primed, but inactive protease that is capable of binding substrates Stp1 and Stp2 (Andréasson *et al.*, 2006; Martins *et al.*, 2018). In effect, the prodomain functions as the inhibitory subunit of the SPS-sensor. In response to amino acids, the prodomain is targeted for degradation by the 26S proteasome, unfettering the catalytically active Cat-domain (Pfirrmann *et al.*, 2010; Abdel-Sater *et al.*, 2011; Omnus *et al.*, 2011; Omnus and Ljungdahl, 2013, 2014). The free Cat-domain cleaves Stp1 and Stp2, enabling their targeting to the nucleus where they bind to promoters and activate the expression of SPS-sensor–regulated genes (Andréasson and Ljungdahl, 2002; Andréasson, 2004; Wielemans *et al.*, 2010; Tumusiime *et al.*, 2011; Omnus and Ljungdahl, 2014).

Stp1 and Stp2 (Stp1/2) are synthesized as latent precursors excluded from the nucleus by negative regulatory activities intrinsic to their N-terminal domains. Two sequence motifs within the first 125 amino acid residues of Stp1/2, regulatory motifs I (RI) and II (RII), place these transcription factors under SPS-sensor control (Andréasson and Ljungdahl, 2002, 2004; Omnus *et al.*, 2016). The latent forms of Stp1/2 are unable to gain access to SPS-sensor–regulated promoters due to the presence of RI. RII is required for binding the Ssy5 Cat-domain and possesses the endoproteolytic processing site (Andréasson and Ljungdahl, 2004). We have recently reported the precise Ssy5 cleavage site in Stp1, which occurs between cysteine 85 and serine 86 within RII, and described the sequence determinants for substrate processing (Martins *et al.*, 2018). Ssy5 exhibits marked S1 specificity being only able to cleave its substrates when amino acids with short side chains are at the P1 position (position N-terminal to the cleavage site; Martins *et al.*, 2018). Strikingly, RI and RII function in a modular manner and are transferrable (Andréasson and Ljungdahl, 2004, 2014). The N terminus of Stp1 fused with the synthetic transcription factor LexA-AD is subject to amino acid–induced SPS-sensor–dependent processing, converting this normally constitutively nuclear-localized activator (Rhee *et al.*, 2000) into a latent cytoplasmic and fully SPS-sensor–regulated factor. Furthermore, the Stp1 N-terminal region is able to control the localization of histone Htb2, a protein that normally efficiently targets to the nucleus, also placing it under SPS-sensor control (Omnus and Ljungdahl, 2014).

The current knowledge regarding SPS-sensor activation suggests that Ssy5 proteolytically activates Stp1/Stp2 in close proximity to the PM. Ssy5 is predicted to be a soluble protein; however, it is peripherally associated with the PM (Forsberg and Ljungdahl, 2001) and a core part of the PM-localized SPS-sensor (Bernard and André, 2001; Forsberg and Ljungdahl, 2001; Abdel-Sater *et al.*, 2004). Moreover, the amino acid–induced signaling events that culminate in unfettering the active Cat-domain have been studied in detail and shown to require a close association with the PM (Abdel-Sater *et al.*, 2004, 2011; Liu *et al.*, 2008; Pfirrmann *et al.*, 2010; Omnus *et al.*, 2011; Omnus and Ljungdahl, 2013). The uniquely long cytoplasmically oriented N-terminal domain of Ssy1 functions as a scaffold that facilitates interactions with Ptr3 and Ssy5 (Didion *et al.*, 1998; Jørgensen *et al.*, 1998; Iraqui *et al.*, 1999; Klasson *et al.*, 1999). Ptr3 plays a key role as a dedicated adaptor that links the conformational changes of the Ssy1 receptor to effectively present the Ssy5 prodomain as a substrate of the PM-bound casein kinases Yck1/2, facilitating prodomain phosphorylation (Abdel-Sater *et al.*, 2011; Omnus *et al.*, 2011; Omnus and Ljungdahl, 2013). Phosphorylation serves as a switch-like trigger to recruit the ubiquitin E3 ligase complex SCF^{Grr1}, which leads to the ubiquitylation of the hyperphosphorylated prodomain (Pfirrmann *et al.*, 2010; Abdel-Sater *et al.*, 2011; Omnus *et al.*, 2011) and its subsequent degradation by the 26S proteasome (Pfirrmann *et al.*, 2010; Omnus *et al.*, 2011).

In the absence of inducing amino acids, Stp1/2 display a diffuse cytoplasmic distribution; however, upon induction these transcriptions factors rapidly localize to the nucleus (Andréasson and Ljungdahl, 2002; Omnus and Ljungdahl, 2014). The N terminus of Stp1, amino acids 2–158, is able to direct the human Cdc25 homologue SOS (hSOS) to the PM (Andréasson and Ljungdahl, 2002). The SOS recruitment system exploits the fact that the hSOS can suppress the temperature-sensitive growth defect of a *cdc25-2* strain when it is localized in close proximity to the PM, a property that is dependent on hSOS being fused to a PM-associated partner (Aronheim *et al.*, 1997). In more recent experiments, it was shown that amino acid residues 16–50 of Stp1, containing the RI motif, suffice to localize hSOS to the cytosolic face of the PM (Omnus and Ljungdahl, 2014).

Intriguingly, the active Ssy5 Cat-domain can cleave a mutant form of Stp1 lacking RI, which is not expected to localize at the PM (Omnus and Ljungdahl, 2014). This challenges the idea that Ssy5 processing activity is confined to the PM and raises questions regarding the subcellular distribution of Ssy5. It has been proposed that reversible ubiquitylation of the prodomain, rather than its degradation, may control the proteolytic activity of the Cat-domain. Accordingly, prodomain ubiquitylation could suffice to partially unleash the Cat-domain and regulated deubiquitylation of the prodomain could restore the autoinhibited state (Abdel-Sater *et al.*, 2011). Experimental evidence for this possible regulatory mechanism is lacking. Given what is known regarding Ssy5 activation, once the prodomain has been degraded, the Cat-domain is irreversibly unfettered (Omnus *et al.*, 2011). Thus, cells are likely to possess mechanisms that control unintentional, and potentially destructive, Cat-domain proteolysis.

Here, we have investigated the proteolytic activity of the Ssy5 Cat-domain once unfettered from the inhibitory prodomain. Consistent with the Cat-domain sharing a remarkable degree of structural similarity with the well-studied α-lytic subfamily of secreted bacterial proteases (Martins *et al.*, 2018), the activated Cat-domain is very stable in lysates prepared from amino acid–induced cells. The Stp1 processing activity of the Cat-domain remains robust in lysates maintained at 4°C for up to 1 mo. The active Cat-domain can dissociate from the PM and carry out endoproteolytic processing events at cellular locations distinct from the PM. The Cat-domain is ubiquitylated and exhibits enhanced turnover in amino acid–induced cells. Together our results indicate that cells target the Cat-domain for degradation to reset the SPS-sensor signaling system.

RESULTS

Ssy5 Cat-domain recognizes RII motifs placed out of natural contexts

To critically test the spatial constraints that may impact on the Ssy5 Cat-domain, and its ability to bind and cleave substrates, we tested its ability to recognize and cleave synthetic substrates in which the

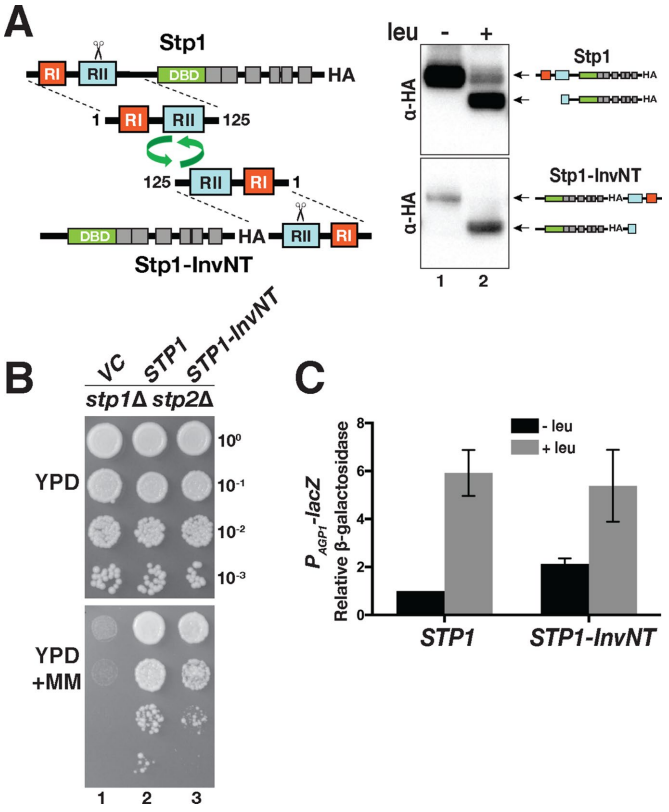

FIGURE 1: The modular N-terminal regulatory domains of Stp1 retain their functional identity when repositioned at the C terminus in an inverted orientation. (A) Schematic representation of Stp1. The location of regulatory regions I (RI) and II (RII), the DNA-binding domains (DBD), and Ssy5 cleavage site (scissors) are indicated. Repositioning Stp1 regulatory regions at the C terminus in a reverse orientation creates an artificial protein Stp1-InvNT; the Ssy5 cleavage site is indicated (scissors). Strain CAY123 (*stp1*Δ*stp2*Δ) carrying the vector pCA047 (*STP1*) or pDO002 (*STP1InvNT*; right panels) was grown in SD medium and cells were harvested 30 min after induction by leucine as indicated; immunoreactive forms of HA-tagged Stp1 species are indicated at their corresponding positions of migration. (B) Growth of strain CAY123 (*stp1*Δ*stp2*Δ) carrying plasmids as in A. Tenfold dilutions of cultures grown in SD were spotted onto YPD and YPD + MM; plates were incubated at 30°C for 2 d and photographed. (C) β-Galactosidase (lacZ) activity in MBY75 (*stp1*Δ*stp2*ΔP_{AGP}-*lacZ*) carrying pCA047 (*STP1*) or pDO002 (*STP1InvNT*) grown in SD in the absence or presence of leucine as indicated. The data ($n = 3$) are normalized to lacZ levels in uninduced (–leu) cells carrying wild-type *STP1*; error bars indicate SD.

regulatory motifs of Stp1 and Stp2 were placed in nonnatural contexts. First, we created an artificial protein with the first 125 residues of Stp1 repositioned in the reverse orientation and placed at the C terminus (Stp1-InvNT; Figure 1A) and assessed whether this protein could be processed by Ssy5 in an SPS-sensor–controlled manner. Upon leucine induction, similar to native Stp1, the Stp1-InvNT construct was readily cleaved (Figure 1A; compare top and bottom panels, respectively). Consistently, the expression of *STP1-InvNT* complemented *stp1*Δ *stp2*Δ growth defects in the presence of MM (2-{[({[(4-methoxy-6-methyl)-1,3,5-triazin-2-yl]-amino}carbonyl) amino-]-sulfonyl}-benzoic acid (Figure 1B, dilution series 3). MM is an inhibitor of branched chain amino acid biosynthesis; cells lacking a functional SPS-sensor are sensitive to MM due to their inability to take up sufficient levels of branched chain amino acids to support growth (Jørgensen *et al.*, 1998). The results show that Stp1-InvNT complemented the *stp1*Δ *stp2*Δ growth phenotype on MM comparably to wild-type (WT) Stp1. These results extend the previous findings on the modular and transferable nature of the N-terminal regulatory domain of Stp1 (Andréasson and Ljungdahl, 2004; Omnus and Ljungdahl, 2014) and demonstrate the robustness of SPS-sensor–dependent regulation of gene expression. These results imply that there is an extremely high affinity between the RII motif of Stp1 and the Ssy5 Cat-domain. Also, the promoter exclusion activity of the RI motif is retained when placed in the inverted C-terminal context; basal, noninduced expression of a Stp1-dependent promoter is low in the absence of amino acid induction (Figure 1C).

Ssy5 Cat-domain cleaves Shr3-Stp1 at the endoplasmic reticulum

According to the current understanding of SPS-sensor–dependent signaling, Ssy5 is activated through signaling events at the PM. It has also been shown that Stp1/Stp2, the only known physiological Ssy5 substrates, are able to interact with the PM. Together these findings suggest that Stp1/Stp2 processing by Ssy5 occurs in close proximity to PM. However, the ability of Cat-domain to find and cleave substrates containing the recognition sequence in a nonnative context (Figure 1), and that engineered substrates carrying RII but not RI are cleaved upon amino acid induction (Omnus and Ljungdahl, 2014), made us question whether Ssy5 activity is confined to the PM. To test this notion, we assessed the ability of Cat-domain to cleave an artificial substrate consisting of Stp1 fused to the cytoplasmic oriented C terminus of the well-characterized endoplasmic reticulum (ER) membrane–localized protein Shr3 (Figure 2A, Shr3-Stp1). Strikingly, the Shr3-Stp1 fusion protein is bifunctional; the construct fully complemented the *shr3*Δ and *stp1*Δ *stp2*Δ growth phenotypes on MM (Figure 2A; compare dilutions 3 and 6 with vector [vc; dilutions 1 and 4] and WT *SHR3* and *STP1* [dilutions 2 and 5, respectively]). The observed growth suggested that Stp1 is correctly processed even when covalently anchored to an integral protein of the ER. To directly test this notion, we monitored the time course of leucine-induced Stp1-myc and Shr3-Stp1-HA (hemagglutinin) processing by immunoblot analysis. In comparison to Stp1, the Shr3-Stp1 fusion protein was processed (Figure 2B, top panels) with equal efficiency and at similar initial rates (Figure 2B, bottom panel).

These results raised the distinct possibility that once unfettered from the inhibitory prodomain, the Ssy5 Cat-domain is able to target to the ER and bind the RII motif of Stp1 and catalyze its cleavage from the Shr3 membrane anchor. We examined the intracellular location of Shr3-Stp1 by subcellular fractionation. Cell lysates were prepared from strain CAY123 (*stp1*Δ *stp2*Δ) expressing *SHR3-STP1* (pSH113) grown on SD in the absence of induction (–leu). The lysates were fractionated on 12–60% step sucrose gradients and analyzed by immunoblotting. Shr3-Stp1 cofractionated with native Shr3 (Figure 2C, top panels), with the highest intensity bands for both proteins in fraction 7, the same fraction as the ER marker protein Dpm1 (dolichol phosphate mannose synthase) and clearly away from Pma1, the PM marker protein (fractions 1–3). To determine the site of Shr3-Stp1 processing, we repeated the subcellular fractionation using extracts prepared from leucine-induced cells (+leu; Figure 2C, bottom panels). Again, the nonprocessed form of Shr3-Stp1 was primarily within fraction 7, colocalizing with the ER marker protein Dpm1. The cleaved form of Stp1 was displaced from the ER and detected in fraction 8. These results strongly suggested that Ssy5 processing activity is not confined to the PM.

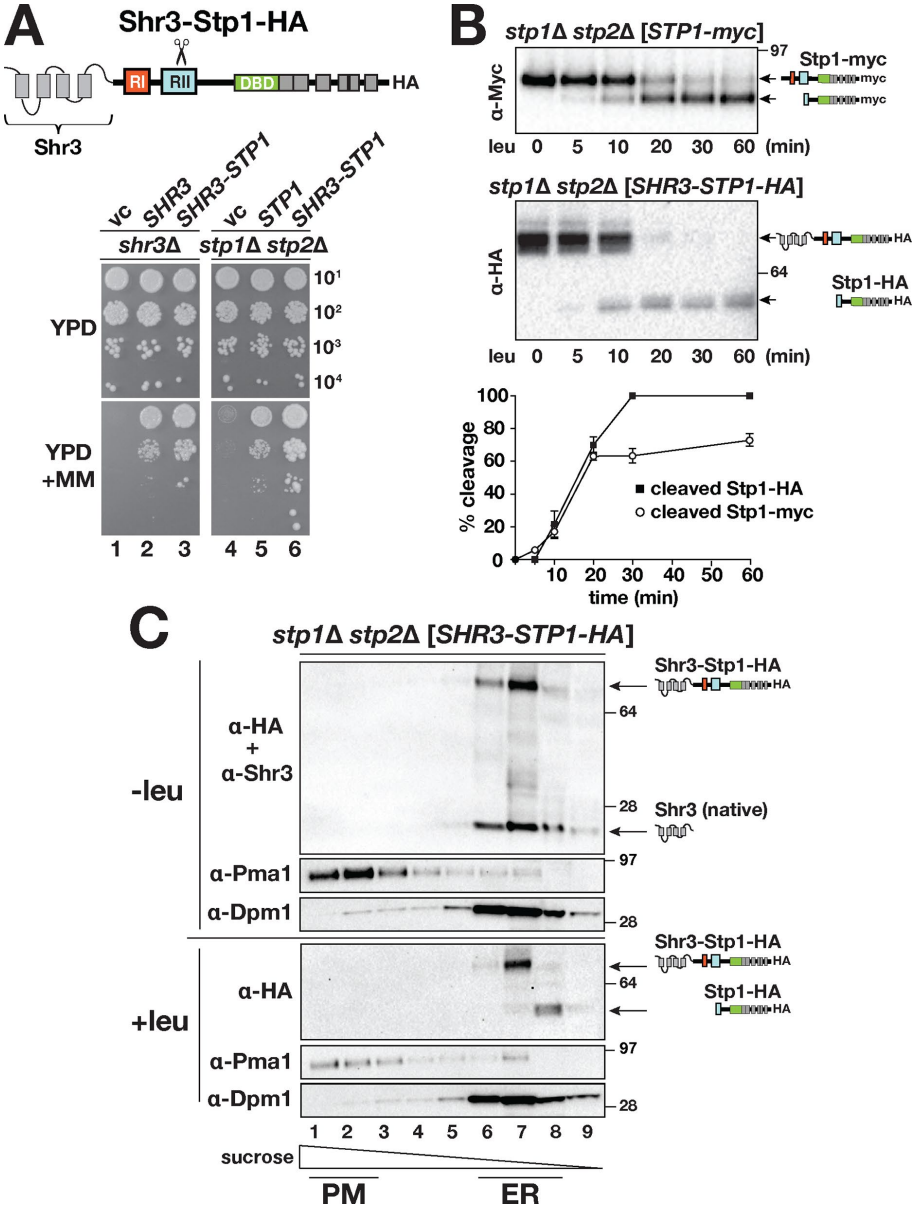

FIGURE 2: The Shr3-Stp1 fusion protein is ER localized and cleaved upon leucine induction. (A) Schematic representation of Shr3-Stp1; the Ssy5 processing site is indicated (scissors). Growth of strains JKY2 (*shr3*Δ) carrying plasmids pRS316 (vector control, vc), pPL210 (*SHR3*), or pSH113 (*SHR3-STP1*; left panel), and CAY123 (*stp1*Δ*stp2*Δ) carrying plasmids pRS316 (vc), pCA211 (*STP1-myc*), or pSH113 (*SHR3-STP1-HA*; right panel). Tenfold dilutions of cultures grown in SD were spotted onto YPD and YPD + MM; plates were incubated at 30°C for 2 d and photographed. (B) SD-grown cultures of CAY123 (*stp1*Δ*stp2*Δ) carrying plasmids pCA211 (*STP1-myc*; top panel) or pSH113 (*SHR3-STP1-HA*; middle panel) were induced with leucine and extracts were prepared at the times indicated and analyzed by immunoblot; immunoreactive forms of Stp1 species are indicated at their corresponding positions of migration. The signal intensities of the cleaved and full-length forms of Stp1 and Shr3-Stp1 were quantified, and the percentage of cleavage was determined (bottom panel; mean values plotted). Error bars show SD ($n = 3$). (C) Shr3-Stp1 cofractionates with Shr3 and Dpm1. Strain CAY123 (*stp1*Δ*stp2*Δ) carrying vector pSH113 (*SHR3-STP1-HA*) was grown in SD and extracts were prepared 30 min after the addition of 1.3 mM leucine (+leu) or water (–leu). The extracts were fractionated on 12–60% sucrose step gradients. Proteins within fractions 1–9 were separated by SDS–PAGE and analyzed by immunoblotting; blots were developed using α-HA and α-Shr3 antibodies as indicated. Antibodies recognizing marker proteins Pma1 and Dpm1 were used to identify fractions containing PM and ER proteins, respectively.

Ssy5 Cat-domain cleaves ER-localized Shr3-Stp1 independent of ER–PM junctions

Based on our results, the unfettered Ssy5 Cat-domain is able to target an ER-localized substrate for cleavage. However, based on knowledge that the ER forms a continuous membrane network throughout the cell (Friedman and Voeltz, 2011) and engages in cross-talk with the PM through cortical ER–PM junctions (Stefan *et al.*, 2013), it is possible that the Ssy5 Cat-domain remains PM associated but engages with the Shr3-Stp1 substrate due to the physical proximity with the ER. To examine this possibility, we obtained a Δtether strain that lacks ER–PM junctions (ANDY198; kind gift of Christopher Stefan, University College London). The Δtether strain carries null alleles of a discrete set of tethering factors (*ist2*Δ *scs2*Δ *scs22*Δ *tcb1*Δ *tcb2*Δ *tcb3*Δ) and exhibits dramatic reductions of the cortical ER network (Manford *et al.*, 2012; Omnus *et al.*, 2016).

We examined the intracellular distribution of Shr3-GFP in WT and Δtether strains (Figure 3A). In comparison to WT cells, which exhibited a well-defined cortical ER network, Δtether cells had clearly altered and collapsed cortical ER. We noted that the Δtether cells were larger and that the Shr3-associated fluorescence exhibited an enhanced perinuclear distribution, consistent with a reduced network of cortical ER. Next, we monitored the processing of Stp1 and Shr3-Stp1 in the Δtether cells. Lysates obtained from Δtether cells carrying pPL1016 (Shr3-Stp1) or pCA211 (Stp1) were examined by immunoblot analysis. The results unequivocally show that leucine rapidly induced the cleavage of Shr3-Stp1 (Figure 3B, bottom left panel) in a manner indistinguishable to Stp1 (Figure 3B, top left panel). By quantifying the levels of processed and full-length forms of Stp1 and Shr3-Stp1, we observed that the cleavage rates were, indeed, very similar for both substrates (Figure 3B, right panel). These results demonstrate that ER–PM tethers are not required for SPS-sensor function, indicating that once activated, Ssy5 is able to engage substrates not located at the PM.

Ssy5 Cat-domain exhibits a disperse intracellular distribution

Although efforts to localize Ssy5 have provided evidence that the two-component "primed" Ssy5 complex, that is, pro- and Cat-domain, interact with the PM (8, 19), the intracellular location of the bulk of

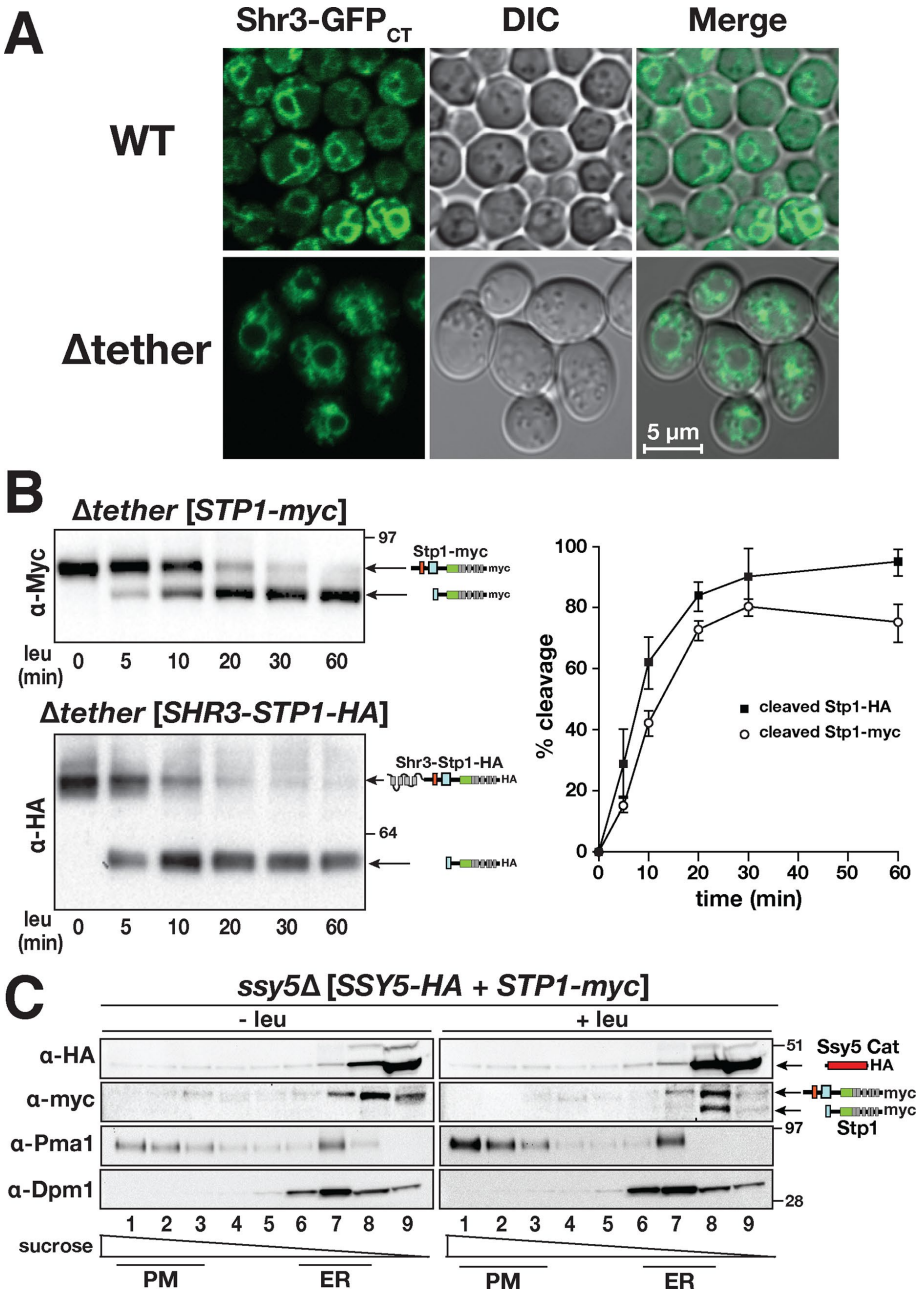

FIGURE 3: Leucine-induced Shr3-Stp1 processing occurs independently of ER–PM junctions. (A) The ER morphology is altered upon loss of ER–PM tethers. Microscopic analysis of WT (SEY6210.1) and Δtether (ANDY198; *ist2*Δ*scs2*Δ*scs22*Δ*tcb1*Δ*tcb2*Δ*tcb3*Δ) strains carrying plasmid pAR046 (*SHR3-GFP*$_{CT}$). Cells were observed by fluorescence microscopy (Zeiss LSM800, 63× objective, DIC, and GFP filters). Scale bar = 5 μm. (B) Leucine-induced processing of Shr3-Stp1. SD + Lys–grown cultures of Δtether strain carrying plasmids pCA211 (*STP1-myc*; top panel) or pSH113 (*SHR3-STP1-HA*; bottom panel). Extracts prepared from subsamples of each culture removed at the indicated time after leucine addition were analyzed by immunoblotting. The signal intensities of the immunoreactive forms of Stp1-myc and Shr3-Stp1-HA were quantified. The percentage of cleavage was determined at the different time points and the mean values plotted (right panel). Error bars show SD ($n = 3$). (C) Ssy5 has dispersed localization and colocalizes with its substrate Stp1. Cells from strain HKY77 (*ssy5*Δ) carrying vector pCA177 (*SSY5-HA*) and pCA204 (*STP1-myc*) were grown in SD. Cell lysates were prepared 30 min after the addition of leucine (+leu; right panel) or an equal volume of water (–leu; left panel), and fractionated on 12–60% step sucrose gradients. Proteins within fractions 1–9 were separated by SDS–PAGE and analyzed by immunoblotting. The antibodies recognizing marker proteins Pma1 and Dpm1 were used to identify fractions containing PM and ER proteins, respectively.

Ssy5, and more specifically the Cat-domain has not been defined. Subcellular fractionation was used to analyze lysates prepared from uninduced and leucine-induced cells. Our focus was on the C-terminal HA epitope–tagged catalytic domain of Ssy5 (Ssy5 Cat) and the substrate Stp1. Cell lysates from strain HKY77 (*ssy5*Δ) expressing Ssy5-HA (pCA177) and Stp1-myc (pCA204) were prepared and fractionated. Immunoblot analysis revealed that both Ssy5 and Stp1 exhibit a disperse and overlapping fractionation pattern (Figure 3C). The highest intensity bands, for both proteins, were in the lighter fractions, corresponding to fractions with largely soluble proteins (Figure 3C; fractions 8 and 9). However, both Cat-domain and Stp1 were present at low levels in heavier fractions (Figure 3C; fractions 3–7). Induction with leucine did not alter the fractionation profile of either protein. As in uninduced cells, the highest levels of processed and nonprocessed Stp1 and the Cat-domain were observed in lighter fractions, with the peak intensity coinciding in fractions 8 and 9 (Figure 3C). These results suggest that the Cat-domain, although having a disperse distribution, is largely soluble or very loosely membrane associated. Although the distribution of the Cat-domain can explain its ability to access substrates away from the PM, it raises the significant question as to how cells control and turn off its proteolytic activity, a requisite for resetting the SPS signaling system. This represents a real conundrum for cells because the prodomain, the only known inhibitor of the Cat-domain enzymatic activity, is degraded in response to amino acid induction. There must be alternative mechanisms to rein in the activity of the Cat-domain, a clear requisite to reset SPS-sensor signaling.

Ssy5 Cat-domain is subject to posttranslational modification in a Ptr3- and Yck1/2-dependent manner

In considering the question of how cells turn off the proteolytic activity of the unfettered Cat-domain, we took note of consistent observations that the Cat-domain appears to be subject to a posttranslational modification. Posttranslational modification of proteases is common and often associated with regulatory mechanisms that modulate their proteolytic activity (López-Otín and Bond, 2008). As a consequence of amino acid induction, the Ssy5 prodomain is extensively modified by phosphorylation in an Yck1/2- and Ptr3-dependent manner, and subsequently ubiquitylated by

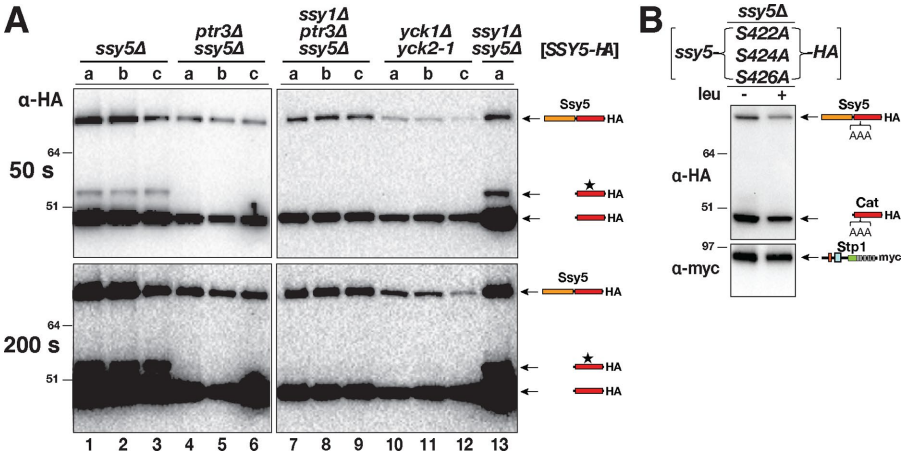

FIGURE 4: Ssy5 Cat is posttranslationally modified in a Ptr3- and Yck1/2-dependent manner. (A) Immunoblot analysis of extracts from three independent biological replicates (a–c) of SD + Lys–grown *ssy5*Δ (HKY77), *ssy5*Δ*ptr3*Δ (HKY85), *ssy5*Δ*ptr3*Δ*ssy1*Δ (CAY285), yck1Δ*yck2-1* (CAY320), and *ssy5*Δ*ssy1*Δ (HKY84) carrying pCA177 (*SSY5-HA*). All strains were grown at 30°C with the exception of *yck1*Δ*yck2-1* (CAY320) grown at room temperature. Blots were exposed 50 s (top panels) and 200 s (bottom panels) as indicated. (B) The Ssy5 Cat-domain modification is dependent on three conserved serine residues. HKY77 (*ssy5*Δ) carrying pAM146 (*ssy5*-S422A, S424A, S426A-HA) and pCA204 (*STP1*-myc) were grown on SD and extracts were prepared 30 min after addition by leucine (+leu) or an equal volume of water (−leu). The immunoreactive forms of HA-tagged Ssy5 and myc-tagged Stp1 are schematically represented at their corresponding positions of migration.

the SCF^{Grr1} E3 ubiquitin ligase (Abdel-Sater *et al.*, 2011; Omnus *et al.*, 2011).

To examine the significance of the observed modification, lysates were prepared from *ssy5*Δ, *ssy5*Δ *ptr3*Δ, *ssy5*Δ *ptr3*Δ *ssy1*Δ, *yck1*Δ *yck2-1*, and *ssy5*Δ *ssy1*Δ strains expressing Ssy5-HA (pCA177) and the migration of the Cat-domain was monitored by immunoblot (Figure 4A). A slower migrating species of Ssy5 Cat-domain was present in extracts from strains *ssy5*Δ and *ssy5*Δ *ssy1*Δ (lanes 1–3 and 13, respectively). The modified Cat-domain was consistently lacking in extracts from *ssy5*Δ *ptr3*Δ and *ssy5*Δ *ptr3*Δ *ssy1*Δ strains (lanes 4–6 and 7–9, respectively). These results indicate that Cat-domain modification occurs in the absence of Ssy1, but is dependent on Ptr3. Similar results were obtained with a Ssy5 allele harboring a C-terminal GST-tag (unpublished data).

The presence of the modified Cat-domain was also dependent on WT Yck1/2 kinase activity. The slower migrating Cat-domain species was lacking in extracts prepared from the temperature-sensitive *yck1*Δ *yck2-1* strain (Figure 4A, lanes 10–12), even when grown at room temperature (RT), a temperature nominally permissive for growth. There was no evidence of Cat-domain modification when the exposure time during immunodetection was substantially increased (4×; bottom panels). Thus, as observed for the Ssy5 prodomain, the Cat-domain is modified by a mechanism coupled to the PM-anchored Yck1/2 kinases.

Ssy5 Cat-domain modification is impaired by mutations in the conserved PISMSLS motif (amino acids 420–426)

The finding that Cat-domain modification is dependent on Yck1/2 prompted us to search for putative phosphorylation sites. The NetPhos 3.1 program (Blom *et al.*, 2004) identified multiple putative phosphorylation sites. Three of these, S422, S424, and S426, are within the highly conserved PISMSLS sequence motif (amino acids 420–426) previously shown to be essential for Ssy5 proteolytic activity. The deletion of five residues in this sequence ($Ssy5^{\Delta PISMS}$) impairs autolytic cleavage and Stp1 processing activity (Abdel-Sater *et al.*, 2004). To test whether serine residues S422, S424, and S426 are phosphorylation acceptor sites, we created a Ssy5 mutant with these residues replaced with alanine (Figure 4B; S422A, S424A, and S426A). Strikingly, the mutations did not affect autolytic processing of Ssy5; the unmodified Cat-domain was clearly evident (Figure 4B, top panel). Hence, this motif is not essential for maturation of the catalytic activity of Ssy5. However, despite being catalytically competent, the mutant Cat-domain lacked leucine-induced Stp1 processing activity (Figure 4B, bottom panel). These results suggest that the three serine residues are important for Ssy5 function in the context of SPS-sensor signaling. The replacement of all three serine residues (S422, S424, and S426) with aspartate, a phosphomimic amino acid, resulted in similar phenotypes as the alanine substitutions; the Ssy5 aspartate mutant exhibited unimpaired autolytic cleavage, but was unable to process Stp1 in response to leucine addition (unpublished data). Consistent with the inability of aspartate substitutions to act in a phosphomimetic manner, alkaline phosphatase treatment did not affect the mobility of the modified Cat-domain (unpublished data). Together these results suggested that the observed modification of the Cat-domain is not simply due to phosphorylation.

Ssy5 Cat-domain is ubiquitylated

The modified Cat-domain migrated with an apparent increase in molecular mass of ≈7 kDa, which prompted us to test whether the observed mobility shift was due to ubiquitylation. Lysates, prepared from cells (HKY77) carrying pCA177 (*SSY5-HA*) grown in SD + Lys (noninducing conditions), were incubated with an anti-HA affinity matrix. The immunoprecipitated proteins were analyzed by immunoblotting developed with α-HA and α-Ubi antibodies (Figure 5). The slower migrating modified species of the Cat-domain was readily detected (α-HA, lane 1) and found to be ubiquitylated (α-Ubi, lane 3).

Next, we addressed the biological significance of the modification and whether it was correlated with amino acid induction. The HA-tagged Cat-domain was immunoprecipitated from lysates prepared from SD + Lys–grown cells induced 60 min with 1.3 mM leucine in the presence of cycloheximide (100 μg/ml). The latter was added to block de novo synthesis, which enabled the apparent stability of the modified Cat-domain to be assessed. In contrast to precipitates from uninduced cells, the precipitates from induced cells did not contain slower migrating forms of the Cat-domain (Figure 5, α-HA, lane 2), and consistently, no ubiquitylation was observed (α-Ubi, lane 4).

The veracity of these observations was critically evaluated by expressing N-terminal hexahistidine-tagged ubiquitin (6xHis-Ubi; Ling *et al.*, 2000) in HKY77 (*ssy5*Δ) carrying *SSY5-HA* together with pPL1307 (+, P_{CUP1}-*6xHIS-Ubi*) or a *LYS2* vector control (vc). Lysates were immunoprecipitated with HA affinity matrix and the mobility of the Cat-domain was analyzed by blotting with α-HA and α-His antibodies (Figure 5, lanes 5–8). Consistent with ubiquitylation, the modifed Cat-domain species exhibited an increased apparent

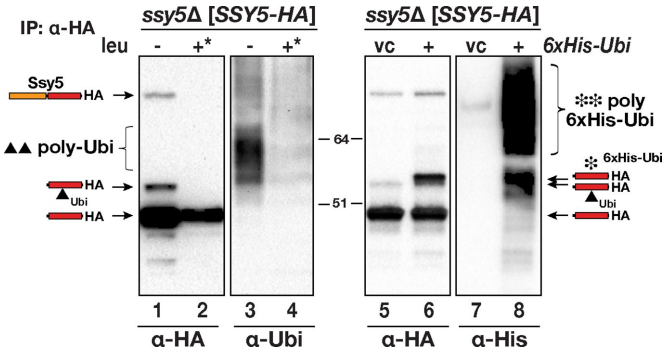

FIGURE 5: The Ssy5 Cat-domain is modified by ubiquitylation. HKY77 (*ssy5*Δ) carrying pCA177 (*SSY5-HA*) alone (lanes 1–4), and together with pRS317 (vc) or pPL1307 (+, P_{CUP1}-*6xHIS-Ubi*; lanes 5–8) was grown in SD and induced with leucine in the presence of 100 μg/ml CHX (+*, lanes 2 and 4) as indicated. Ssy5-HA in extracts was precipitated using an α-HA affinity matrix, and the precipitates were analyzed by immunoblotting; the blots were developed with α-HA (lanes 1–2, 5–6), α-Ubi (lanes 3–4), and α-His (lanes 7–8) antibodies. The migration of the mono- and polyubiquitylated (brackets) Cat-domain species are marked.

molecular mass in cells expressing 6xHis-Ubi (compare lanes 5 and 6). Incorporation of 6xHis-Ubi was confirmed by blotting with α-His antibodies (compare lanes 7 and 8). These results clearly indicate that the Cat-domain is subject to ubiquitylation and suggested that amino acid–induced signals, presumably mediated at the PM in association with the SPS-sensor, affect Cat-domain ubiquitylation.

Ssy5 Cat-domain exhibits remarkable stability in cell lysates

Ssy5 protease activity can be assayed in cell-free lysates in a manner that faithfully reproduces SPS-sensor signaling (Andréasson *et al.*, 2006; Martins *et al.*, 2018). Briefly, protein lysates from *ssy5*Δ *stp1*Δ *stp2*Δ *prb1*Δ cells that express either Stp1-myc or Ssy5-HA are combined, and Stp1 processing is monitored by immunoblotting. Stp1 cleavage is observed only if the Ssy5-HA expressing strain has been induced with leucine before lysate preparation. We prepared leucine-activated lysates and assessed the stability of the Stp1 cleavage activity over an extended period of time. The lysates were maintained at 4°C and the Stp1 cleavage activity was assessed on 0, 15, and 30 d of storage (Figure 6A). The Stp1-containing lysates were prepared freshly to provide the substrate. The results show that Ssy5-Cat is remarkably stable. Stp1-processing activity was readily observed, albeit at a diminished rate, even after 30 d of storage at 4°C (Figure 6A, lanes 11–15). These results strongly suggest that cells possess active mechanisms to down-regulate Cat-domain activity, a requisite for resetting the signaling capacity of the SPS-sensing pathway.

Ssy5 Cat-domain is degraded upon amino acid induction

The inherent stability of the activated Cat-domain in lysates from leucine-induced cells (Figure 6A) is consistent with our previous findings (Pfirrmann *et al.*, 2010), which demonstrated that in contrast to the prodomain, the Cat-domain is relatively stable during the first 45 min of leucine induction. Importantly, in our previous studies, no differences in Cat-domain levels were detected in extracts prepared from non- and amino acid–induced extracts. We revisited these results and critically tested the stability of Ssy5-Cat by performing time-course experiments over an extended time frame in the presence of cycloheximide (CHX). Specifically, we monitored the levels of Ssy5-Cat and full-length Ssy5 over a 90-min period (Figure 6B). The levels of full-length Ssy5 displayed a similar rate of decay independent of induction. This likely reflects that the Ssy5 autolytic event, which occurs constitutively during biogenesis, cleaves the prodomain from the Cat-domain. Hence, Ssy5 autolysis is unaffected by CHX, and the autolysis of already translated Ssy5 is not impaired under the experimental conditions. By contrast, in the absence of amino acid induction, the Cat-domain and the ubiquitylated form of the Cat-domain were stable over the entire 90-min time course (Figure 6B, top left panel, lanes 1–7). Strikingly, leucine induction resulted in reduced levels of the Cat-domain, particularly evident after 45 min (Figure 6B, top right panel, lanes 8–14). Also, the band corresponding to the modified Cat-domain exhibited an enhanced turnover upon leucine induction (Figure 6B, compare left and right panels), and was barely detectable after 45 min. Consequently, the Cat-domain appears to be less stable in amino acid–induced cells. The enhanced degradation of the Cat-domain upon leucine induction indicates that cells target the activated Cat-domain for degradation. These observations, obtained in a strain carrying the *prb1*Δ allele, indicate that the leucine-induced turnover of Cat-domain occurs independently of protein degradation in the vacuole.

DISCUSSION

Proteolytic activation of substrates is irreversible, a fact that makes understanding protease-dependent signaling events inherently interesting. Here we have investigated spatial and temporal aspects of Ssy5 endoprotease function. In response to extracellular amino acids, the activated Ssy5 Cat-domain can recognize and efficiently cleave substrates carrying the Stp1 RI regulatory motif at sites distant from the PM. An ER membrane–anchored protein substrate, Shr3-Stp1, was cleaved in a strain lacking ER–PM tethers, indicating that after degradation of the inhibitory prodomain, the activated Cat-domain can dissociate from the PM. As we have previously reported, Cat-domain levels, relative to the prodomain, are stable under both inducing and noninducing conditions (Pfirrmann *et al.*, 2010). Consequently, to control spurious and perhaps deleterious proteolytic processing events, cells need to overcome the stability and dispersed distribution of the Cat-domain. Clearly, reining in the unfettered Cat-domain is requisite to restore the signaling capacity of the SPS-sensor signaling system. Consistent with this notion, we discovered that the Cat-domain exhibits enhanced turnover in amino acid–induced cells. These results provide the first evidence for how cells reset the signaling competence of the SPS-sensor and extracellular amino acid–induced signaling. Our findings are important for understanding the SPS-sensing system and indicate that subsequent to its biogenesis, Ssy5 function can be assigned to four discrete processes, schematically summarized in Figure 7.

Unlike most proteases, where autolytic processing leads to activation, autolysis of the Ssy5 zymogen into N-terminal pro- and C-terminal Cat-domains does not suffice to activate cleavage of substrate proteins. After autolysis, the prodomain remains noncovalently attached to the Cat-domain and functions as a potent inhibitor of its activity (Andréasson *et al.*, 2006; Poulsen *et al.*, 2006). The unfettering of the catalytic activity of Ssy5 is initially controlled by receptor-activated proteolysis (RAP; Figure 7, process 1; Andréasson *et al.*, 2006); the binding of extracellular amino acids to Ssy1, initiates a series of conformational changes within the SPS-sensor that culminate in the phosphorylation, ubiquitylation, and subsequent proteasomal degradation of the inhibitory Ssy5 prodomain (Omnus *et al.*, 2011). Prodomain degradation unfetters Cat-domain, irreversibly turning on its Stp1- and Stp2-processing activity. The RAP mechanism is distinct from other

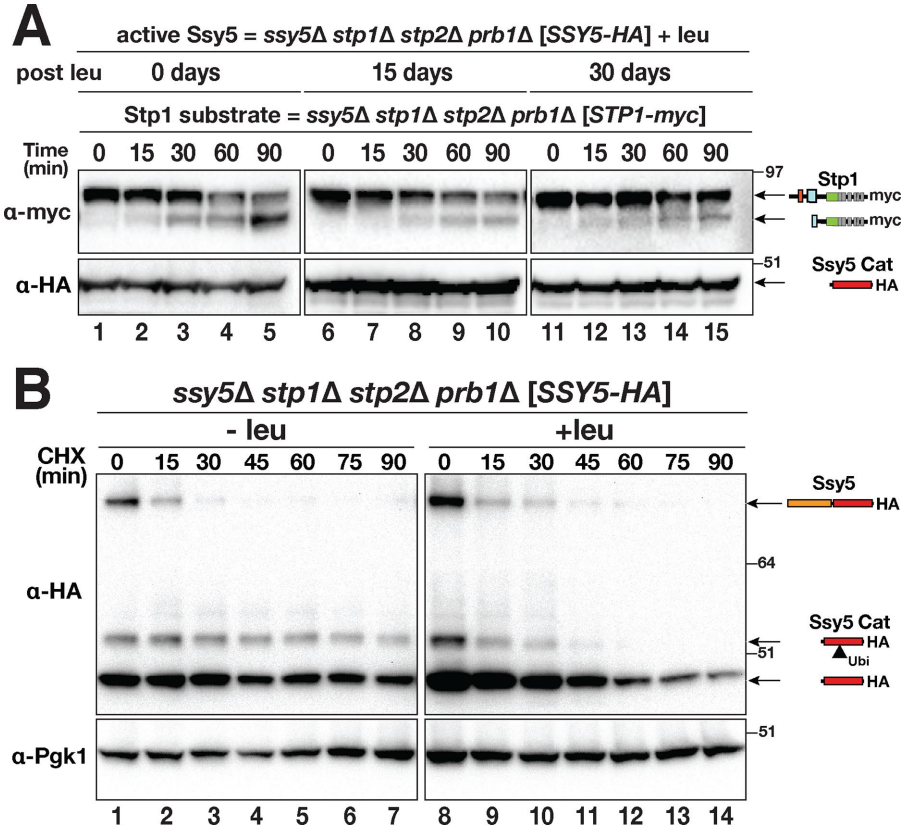

FIGURE 6: Amino acid induction promotes degradation of the Ssy5 Cat-domain. (A) Cat-domain stability in cell-free extracts. Cell lysates of strain AMY001 (*ssy5Δstp1Δstp2Δprb1Δ*) carrying pCA177 (*SSY5-HA*) were prepared 30 min after induction with 1.3 mM leucine and the lysates were stored on ice for the indicated days. Freshly prepared lysates from AMY001 expressing Stp1-myc (pCA211) were mixed, and the cleavage of Stp1 was monitored over a 90-min time course. The immunoreactive forms of myc-tagged Stp1 and HA-tagged Ssy5 Cat are schematically represented at their corresponding positions of migration. (B) Ssy5 Cat-domain stability in strain AMY001 expressing *SSY5-HA* (pCA177). Cells were pregrown in SD and the culture was split into two equal volumes. At $t = 0$ the subcultures received an aliquot of CHX (final concentration equal to 100 µg/ml) and leucine (1.3 mM final concentration; +leu) or an equal volume of water (–leu) as indicated. Cell extracts were subsequently prepared from subsamples removed at the indicated times. The immunoreactive forms of HA-tagged Ssy5 are schematically represented at their corresponding positions of migration. Levels of Pgk1 served as an internal control for protein loading.

characterized signaling pathways involving regulated proteolysis. For example, RIP (regulated intramembrane proteolysis) and RUP (regulated ubiquitin/proteasome-dependent processing) rely on mediating effector substrate availability rather than by direct regulation of a protease (Brown *et al.*, 2000; Hoppe *et al.*, 2000, 2001; Stöven *et al.*, 2003).

In the course of our investigations, we discovered that the Cat-domain is a substrate for a posttranslational modification. The observed modification, which to our knowledge has not previously been reported, was found to be dependent on Ptr3 and the PM-bound casein kinases Yck1/2. These components are known to be required for Ssy5 prodomain hyperphosphorylation (Omnus *et al.*, 2011). Curiously, although Ssy5 prodomain and Ptr3 hyperphosphorylation is strictly dependent on Ssy1, the Cat-domain modification was evident in a strain lacking Ssy1. Amino acid binding to Ssy1 is thought to stabilize a signaling conformation of Ptr3 that provides a binding surface for Yck1/2, with Ptr3 playing a critical role in recruiting the kinase into spatial proximity of Ssy5 (Omnus and Ljungdahl, 2013). Ssy5 and Ptr3 have been shown to interact independently of Ssy1, and on the basis of our new results, Ptr3 may interact with Yck1/2 independently of Ssy1. It has been speculated that Ptr3 and Ssy5 comprise a subcomplex within the SPS-sensor (Bernard and André, 2001; Liu *et al.*, 2008; Omnus and Ljungdahl, 2013). Intriguingly, although a fraction of the Cat-domain is ubiquitylated in the absence of amino acid induction, this fraction appears to be relatively stable under noninducing conditions. This finding suggests that in the context of the "primed-form" of Ssy5, in which the Cat-domain is tightly associated with the prodomain (Andréasson *et al.*, 2006), the ubiquitylated Cat-domain is refractory to degradation. Upon amino acid induction, which promotes prodomain degradation, the ubiquitylated Cat-domain is subject to degradation (Figure 6B).

We investigated the intracellular location of Ssy5 by subcellular fractionation and found that Ssy5 Cat-domain presents a dispersed distribution. The intracellular localization of the Cat-domain did not change in the presence of inducing amino acids. Ssy5 colocalizes with its substrate Stp1, consistent with the definition of a physiological substrate for a protease (Turk *et al.*, 2012), and is more abundant in fractions containing soluble proteins. To test the significance of the dispersed distribution of the Cat-domain we constructed an artificial ER membrane–bound substrate (Shr3-Stp1). Strikingly, this substrate was subject to amino acid–induced proteolysis with the same kinetics as native Stp1 and occurred in a strain lacking ER–PM tethers (Δtether). Clearly, amino acid–induced Ssy5 activation and cleavage of the ER-localized Shr3-Stp1 fusion protein occurs independently of tethering. The implication of this finding is that the catalytic activity of Ssy5 is not limited to the PM; once activated, the unfettered Cat-domain dissociates and efficiently binds substrates at sites distant from the cell periphery (Figure 7, process 2).

Consistent with our previous undocumented results (Martins *et al.*, 2018), the activated Cat-domain exhibited a high degree of stability; extracts prepared from amino acid–induced cells lacking Stp1 and Stp2 retained the ability to cleave Stp1 even after 1 mo of storage at 4°C. The in vitro assay provided a clear demonstration of the high intrinsic stability of the activated Cat-domain, and demonstrates the catalytic cycle of substrate binding and cleavage (Figure 7, processes 3a and 3b). Considering the consequences of an inherently stable protease with a dispersed intracellular distribution and a high affinity for substrates, we sought to define the regulatory mechanisms that control the activated Cat-domain. We tested the in vivo stability of the Cat-domain, extending the time course to 90 min, and observed that amino acid–induction stimulated Cat-domain degradation. These results indicate that amino acid–induced degradation of the Cat-domain provides the means to reset the capacity of yeast cells to sense and respond to extracellular amino acids (Figure 7, process 4). The mechanisms underlying the

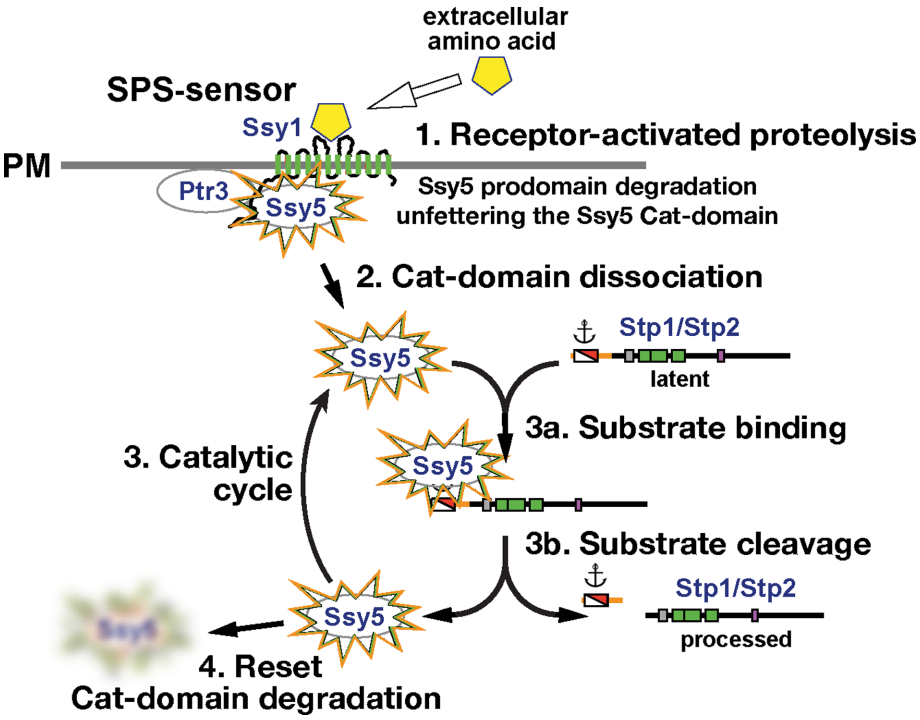

FIGURE 7: Schematic of Ssy5 Cat-domain activation, catalytic role, and degradation. Subsequent to its biogenesis and autolytic processing, the control and function of the Ssy5 Cat-domain can be described within the context of the four indicated processes.

turnover of the unfettered Cat-domain need to be further defined, but we note that it is unlikely to involve SPS-sensor–derived signals; Ssy5-HA has been shown to be degraded at similar rates in *ssy5Δ*, *ssy1Δ ssy5Δ*, and *ptr3Δ ssy5Δ* strain backgrounds when cells are grown under inducing conditions in the presence of amino acids (Liu *et al.*, 2008).

Finally, we note that the SPS-sensing pathway can be exploited to study the spatial requirements and specific localization of diverse catalytic events. The modularity and transferability of Stp1 N-terminal RI and RII has previously been reported (Andréasson and Ljungdahl, 2004; Omnus and Ljungdahl, 2014), but we now possess the means to control the Cat-domain and specifically cleave ER-localized and membrane-anchored substrates. This greatly expands the technical repertoire for using the SPS-sensing pathway as a system for controlling the intracellular localization of proteins in yeast. The ability to anchor soluble proteins to the ER membrane and to rapidly liberate them has advantages over existing sequestration systems (Haruki *et al.*, 2008). For example, the activity of nuclear components, specifically involved with transcription, chromatin remodeling, or recombination, can be placed under the control of the SPS-sensor by constructing fusions containing the RII regulatory motif of Stp1 placed at the C terminus to Shr3. Thus, access of individual proteins to the nucleus can be effectively restricted, and their localization controlled in a highly regulated manner merely by the addition of a single amino acid. This may be useful in testing the temporal function and physiological consequences of redirecting and sequestering presumed nuclear factors to the cytosolic compartment.

MATERIALS AND METHODS

Strains and plasmids

The construction of all *S. cerevisiae* strains has been documented elsewhere, as indicated (Table 1). With the exception of the Δtether strain, ANDY198 (Manford *et al.*, 2012), and its WT strain, SEY6210.1 (obtained from the Christopher Stefan laboratory; Robinson *et al.*, 1988), all strains are isogenic descendants of the S288C-derived strain AA255/PLY115 (Antebi and Fink, 1992). The plasmids used in this work are listed in Table 2. The sequences of mutagenic oligonucleotides and PCR primers for homologous recombination are available upon request.

Media

Standard media, including yeast extract–peptone–dextrose (YPD) medium, ammonia-based synthetic minimal dextrose (SD) medium, supplemented as required to enable growth of auxotrophic strains, and ammonia-based synthetic complete dextrose (SC) were prepared as described previously (Andréasson and Ljungdahl, 2002).

Strain	Genotype	Reference/source
SEY6210.1	*MAT**a** leu2-3,112 ura3-52 his3Δ200 trp1-Δ901 lys2-801 suc2Δ9*	Robinson *et al.*, 1988
ANDY198	SEY6210.1 *ist2Δ::HISMX6 scs2Δ::TRP1 scs22Δ::HISMX6 tcb1Δ::KANMX6 tcb2Δ::KANMX6 tcb3Δ::HISMX6*	Manford *et al.*, 2012
AMY001	*MAT**a** ura3-52 ssy5Δ1::hisG stp1Δ51::Agleu2 stp2Δ50::hphMX4 prb1Δ::kanMX*	Martins *et al.*, 2018
CAY123	*MAT**a** ura3-52 stp1Δ51::Agleu2 stp2Δ50::hphMX4*	Andréasson and Ljungdahl, 2002
CAY285	*MAT**a** lys2Δ201 ura3-52 ptr3Δ15::hisG ssy1Δ13::hisG ssy5Δ2::hisG*	Andréasson *et al.*, 2006
CAY320	*MAT**a** lys2Δ201 ura3-52 yck1Δ::hphMX4 yck2-1*	Omnus *et al.*, 2011
HKY77	*MAT**a** lys2Δ201 ura3-52 ssy5Δ2::hisG*	Forsberg and Ljungdahl, 2001
HKY84	*MAT**a** lys2Δ201 ura3-52 ssy1Δ13::hisG ssy5Δ2::hisG*	Forsberg and Ljungdahl, 2001
HKY85	*MAT**a** lys2Δ201 ura3-52 ptr3Δ15::hisG ssy5Δ2::hisG*	Forsberg and Ljungdahl, 2001
JKY2	*MAT**a** ura3-52 shr3Δ6*	Ljungdahl laboratory strain
MBY75	*MAT**a** ura3-52 stp1Δ51::Agleu2 stp2Δ50::hphMX4 gap1Δ::*P_{AGP1}*-lacZ*	Ljungdahl laboratory strain

TABLE 1: Yeast strains used in this study.

Plasmid	Description of insert in pRS316 (*URA3*)	Reference
pAM146	*SSY5(S422A,S424A,S226A)-6xHA-KlTRP1*	This work
pCA047	*STP1-3xHA*	Andréasson and Ljungdahl, 2002
pCA177	*SSY5-6xHA-KlTRP1*	Andréasson *et al.*, 2006
pCA204	*STP1-13xMYC-kanMX*	Andréasson *et al.*, 2006
pCA211	*STP1-13xMYC-kanMX*	Andréasson *et al.*, 2006
pDO002	*STP1*($\Delta_{1\text{-}125}$)*-3xHA-R2R1*	This work
pPL210	*SHR3*	Ljungdahl *et al.*, 1992
pPL1307	YEp195-based (2μ, *URA3* replaced with *LYS2*) containing P_{CUP1}*-6xHIS-Ubi*	Omnus *et al.*, 2011; Davies and Ulrich, 2012
pSH113	*SHR3-STP1-3xHA*	This work
pAR046	*SHR3-GFP*$_{CT}$	This work

TABLE 2: Plasmids used in this study.

When needed, L-leucine was added at a concentration of 1.3 mM to induce SPS-sensor signaling. Sensitivity to MM (2-{[({[(4-methoxy-6-methyl)-1,3,5-triazin-2-yl]-amino}carbonyl)amino-]-sulfonyl}-benzoic acid) on complex medium is described elsewhere (Andréasson and Ljungdahl, 2004).

Immunoblot analysis

Whole-cell extracts were prepared under denaturing conditions as described previously (Silve *et al.*, 1991). Primary mouse monoclonal antibodies were diluted as follows: anti-myc 9E10 (Roche Applied Science), 1:5000; 3F10 anti-HA-HRP (Roche Applied Science), 1:5000; anti-myc-HRP 9E10 monoclonal antibody (Roche Applied Science), 1:5000; anti-Pgk1 (Abcam), 1:10,000. Where appropriate, goat anti-mouse–poly-HRP (Thermo Scientific; 1:5000) was used for immunodetection. Immunoreactive bands labeled were visualized by chemiluminescence detection (SuperSignal West Dura Extended-Duration Substrate; Thermo Fisher Scientific) of horseradish peroxidase using an LAS1000 system (Fuji Photo Film) or a ChemiDoc imaging system (Bio-Rad). Quantification was performed using ImageLab software (Bio-Rad).

In vitro protease assay

Yeast cells were grown in SD to an OD_{600} of 1. The cultures expressing Ssy5 were induced for 30 min with 1.3 mM leucine. Cells were disrupted by bead beating (3 × 20 s) in lysis buffer (50 mM HEPES-KOH, 100 mM NaCl, 5 mM dithiothreitol [DTT] at pH 8.0), and non-lysed cells were removed by low speed centrifugation (1200 × *g*) for 15 min. Protease reactions were prepared on ice in lysis buffer (pH 7.4) by mixing equal amounts of Stp1 and Ssy5 containing lysate. Reactions were incubated at 30°C for 90 min, stopped by the addition of 2× sample buffer, boiled, and separated on SDS–PAGE.

Subcellular fractionation

Cells were grown on SD at 30°C and harvested when cultures reached an OD_{600} of 0.8, and protein extracts were prepared and fractionated on 12–60% sucrose gradients essentially as described previously (Antebi and Fink, 1992; Egner *et al.*, 1995; Klasson *et al.*, 1999), with some modifications. Specifically, harvested cells were resuspended in 0.5 ml of lysis buffer (0.8 M sorbitol, 10 mM MOPS, pH 7.2, 2 mM EDTA, 1 mM phenylmethylsulfonyl fluoride [PMSF], 1X complete protease inhibitor cocktail; Roche). The cells were lysed by bead beating with 0.5-mm glass beads using 3 × 20 s pulses (6.5 MPS; Fastprep-24 benchtop homogenizer; MP Biomedical). The broken cell suspension was transferred to a 1.5-ml tube and cleared, twice, by centrifuging at 4000 rpm for 5 min. The resulting supernatant was layered onto a step gradient prepared as follows: a 0.5-ml step of 60% (wt/vol) and 1 ml each of 54, 48, 42, 36, 30, 24, 18 and 12% (wt/vol) sucrose in lysis buffer. The gradients were centrifuged for 3 h at 150,000 × *g*. One-milliliter fractions were collected from the bottom of the gradients using a fraction recovery system (Beckman Coulter). Proteins from equal aliquots of the resulting fractions were concentrated by PMSF precipitation. Proteins were separated by SDS–PAGE and blotted onto nitrocellulose membranes. Immunoblots were incubated as indicated with primary antibody; α-Pma1 (Abcam), 1:1000; α-Dpm1 (Abcam), 1:2500; α-Shr3 (Ljungdahl Laboratory), 1:9000; 3F10 anti-HA-HRP (Roche Applied Science), 1:5000; anti-myc-HRP 9E10 monoclonal antibody (Roche Applied Science). Where appropriate, goat anti-rabbit or anti-mouse poly-HRP (Thermo Scientific; 1:5000) were used for immunodetection. Immunoreactive proteins were visualized by chemiluminescence detection of horseradish peroxidase (SuperSignal West Dura Extended-Duration Substrate; Thermo Fisher Scientific) and a ChemiDoc imaging system (Bio-Rad). Each fractionation experiment was repeated using a minimum of three biological replicas; no substantial differences in the distribution of the proteins were observed. The immunoblots in Figures 2C and 3C accurately represent the consistent subcellular fractionation data obtained.

β-Galactosidase activity assay

β-Galactosidase activity was determined with *N*-lauroyl-sarcosine–permeabilized cells (Kippert, 1995). Cells grown in SD were harvested by centrifugation, washed once, and resuspended in 200 μl of Z buffer (60 mM Na_2HPO_4, 40 mM NaH_2PO_4, 10 mM KCl, 1 mM $MgSO_4$, 50 mM β-mercaptoethanol, pH 7), and the OD_{600} was measured. A 40-μl aliquot of cell suspension was mixed with 760 μl of 0.2% (wt/vol) Na *N*-lauroyl-sarcosine Z buffer and incubated at 30°C for 15 min. Then preheated 160 μl of Z buffer containing 4 mg/ml 2-nitrophenyl β-D-galactopyranoside was added. After a 10-min incubation at 30°C, the reaction was quenched by the addition of 400 μl of 1 M Na_2CO_3. Samples were centrifuged at 12,000 × *g* for 5 min, and the absorbance of the supernatant was measured at 420 nm.

Cycloheximide chase

Cells were inoculated at an optical density at 600 nm of 0.5 and grown at 30°C for 3 h. Cycloheximide (CHX) was added to the cells

at a concentration of 100 µg/ml, and where indicated, leucine was added to a concentration of 1.3 mM (+leu). Extracts were prepared from samples taken at the time points indicated and analyzed by immunoblotting.

Immunoprecipitation

Cells were grown on SD + Lys at 30°C, induced with 1.3 mM leu for 60 min in the presence of 100 µg/ml cycloheximide (CHX) as indicated. Cells, corresponding to approximately OD_{600} of 100, were harvested in log phase and resuspended in 250 µl of lysis buffer (0.8 M sorbitol, 10 mM MOPS, pH 7.2, 100 mM NaCl, 2 mM EDTA, 1 mM PMSF, 1X complete protease inhibitor cocktail; Roche Applied Science). Glass beads (0.5 mm) were added, and cells were lysed by bead beating (3 × 20 s pulses; Fastprep-24 benchtop homogenizer, MP Biomedical). The disrupted cell suspension was transferred to a 2-ml tube and cleared by centrifugation at 500 × *g* for 10 min. The resulting supernatant was added to 50 µl of anti-HA affinity matrix (Roche Applied Science) and incubated while rotating for 1 h at 4°C. The beads were washed twice with 500 µl of lysis buffer; tubes were changed between washes. Proteins were eluted by denaturation at 95°C for 5 min in sample buffer and separated by SDS–PAGE and blotted onto nitrocellulose membranes. Immunoblots were incubated as indicated with primary antibody: P4D1 anti-ubiquitin-HRP (Santa Cruz), 1:1000; 3F10 anti-HA-HRP (Roche Applied Science), 1:2500, or anti-6xHis (Clontech), 1:5000. Where appropriate, goat anti-mouse poly-HRP (Thermo Scientific; 1:5000) was used for immunodetection. Immunoreactive proteins were visualized by chemiluminescence detection of horseradish peroxidase (SuperSignal West Dura Extended-Duration Substrate; Thermo Fisher Scientific) and a ChemiDoc imaging system (Bio-Rad).

ACKNOWLEDGMENTS

We thank Christopher Stefan, University College London, for kindly providing the Δtether strain. We thank Meliza Ward and Fitz Gerald Silao for help obtaining the microscopy images examining the ER distribution in WT and Δtether strains. Additionally, we thank the members of the Ljungdahl laboratory for constructive comments throughout the course of this work. This research was supported by funding from the Swedish Research Council, VR.NT Contract no. 2015-04202 (P.O.L.).

REFERENCES

Abdel-Sater F, El Bakkoury M, Urrestarazu A, Vissers S, André B (2004). Amino acid signaling in yeast: casein kinase I and the Ssy5 endoprotease are key determinants of endoproteolytic activation of the membrane-bound Stp1 transcription factor. Mol Cell Biol 24, 9771–9785.

Abdel-Sater F, Jean C, Merhi A, Vissers S, André B (2011). Amino acid signaling in yeast: activation of Ssy5 protease is associated with its phosphorylation-induced ubiquitylation. J Biol Chem 286, 12006–12015.

Andréasson C (2004). Ligand-activated proteolysis in nutrient signaling, Stockholm, Sweden: Karolinska Institutet.

Andréasson C, Heessen S, Ljungdahl PO (2006). Regulation of transcription factor latency by receptor-activated proteolysis. Genes Dev 20, 1563–1568.

Andréasson C, Ljungdahl PO (2002). Receptor-mediated endoproteolytic activation of two transcription factors in yeast. Genes Dev 16, 3158–3172.

Andréasson C, Ljungdahl PO (2004). The N-terminal regulatory domain of Stp1p is modular and, fused to an artificial transcription factor, confers full Ssy1p-Ptr3p-Ssy5p sensor control. Mol Cell Biol 24, 7503–7513.

Antebi A, Fink GR (1992). The yeast Ca^{2+}-ATPase homologue, PMR1, is required for normal Golgi function and localizes in a novel Golgi-like distribution. Mol Biol Cell 3, 633–654.

Aronheim A, Zandi E, Hennemann H, Elledge SJ, Karin M (1997). Isolation of an AP-1 repressor by a novel method for detecting protein-protein interactions. Mol Cell Biol 17, 3094–3102.

Bernard F, André B (2001). Genetic analysis of the signalling pathway activated by external amino acids in *Saccharomyces cerevisiae*. Mol Microbiol 41, 489–502.

Blom N, Sicheritz-Pontén T, Gupta R, Gammeltoft S, Brunak S (2004). Prediction of post-translational glycosylation and phosphorylation of proteins from the amino acid sequence. Proteomics 4, 1633–1649.

Brown MS, Ye J, Rawson RB, Goldstein JL (2000). Regulated intramembrane proteolysis: a control mechanism conserved from bacteria to humans. Cell 100, 391–398.

Davies AA, Ulrich HD (2012). Detection of PCNA modifications in *Saccharomyces cerevisiae*. Methods Mol Biol 920, 543–567.

Didion T, Regenberg B, Jørgensen MU, Kielland-Brandt MC, Andersen HA (1998). The permease homologue Ssy1p controls the expression of amino acid and peptide transporter genes in *Saccharomyces cerevisiae*. Mol Microbiol 27, 643–650.

Egner R, Mahé Y, Pandjaitan R, Kuchler K (1995). Endocytosis and vacuolar degradation of the plasma membrane-localized Pdr5 ATP-binding cassette multidrug transporter in *Saccharomyces cerevisiae*. Mol Cell Biol 15, 5879–5887.

Forsberg H, Ljungdahl PO (2001). Genetic and biochemical analysis of the yeast plasma membrane Ssy1p-Ptr3p-Ssy5p sensor of extracellular amino acids. Mol Cell Biol 21, 814–826.

Friedman JR, Voeltz GK (2011). The ER in 3D: a multifunctional dynamic membrane network. Trends Cell Biol 21, 709–717.

Haruki H, Nishikawa J, Laemmli UK (2008). The anchor-away technique: rapid, conditional establishment of yeast mutant phenotypes. Mol Cell 31, 925–932.

Hoppe T, Matuschewski K, Rape M, Schlenker S, Ulrich HD, Jentsch S (2000). Activation of a membrane-bound transcription factor by regulated ubiquitin/proteasome-dependent processing. Cell 102, 577–586.

Hoppe T, Rape M, Jentsch S (2001). Membrane-bound transcription factors: regulated release by RIP or RUP. Curr Opin Cell Biol 13, 344–348.

Iraqui I, Vissers S, Bernard F, de Craene J-O, Boles E, Urrestarazu A, André B (1999). Amino acid signaling in *Saccharomyces cerevisiae*: a permease-like sensor of external amino acids and F-box protein Grr1p are required for transcriptional induction of the *AGP1* gene, which encodes a broad-specificity amino acid permease. Mol Cell Biol 19, 989–1001.

Jørgensen MU, Bruun MB, Didion T, Kielland-Brandt MC (1998). Mutations in five loci affecting *GAP1*-independent uptake of neutral amino acids in yeast. Yeast 14, 103–114.

Khan AR, James MN (1998). Molecular mechanisms for the conversion of zymogens to active proteolytic enzymes. Protein Sci 7, 815–836.

Kippert F (1995). A rapid permeabilization procedure for accurate quantitative determination of β-galactosidase activity in yeast cells. FEMS Microbiol Lett 128, 201–206.

Klasson H, Fink GR, Ljungdahl PO (1999). Ssy1p and Ptr3p are plasma membrane components of a yeast system that senses extracellular amino acids. Mol Cell Biol 19, 5405–5416.

Ling R, Colon E, Dahmus ME, Callis J (2000). Histidine-tagged ubiquitin substitutes for wild-type ubiquitin in *Saccharomyces cerevisiae* and facilitates isolation and identification of in vivo substrates of the ubiquitin pathway. Anal Biochem 282, 54–64.

Liu Z, Thornton J, Spirek M, Butow RA (2008). Activation of the SPS amino acid-sensing pathway in *Saccharomyces cerevisiae* correlates with the phosphorylation state of a sensor component, Ptr3. Mol Cell Biol 28, 551–563.

Ljungdahl PO, Daignan-Fornier B (2012). Regulation of amino acid, nucleotide, and phosphate metabolism in *Saccharomyces cerevisiae*. Genetics 190, 885–929.

Ljungdahl PO, Gimeno CJ, Styles CA, Fink GR (1992). SHR3: a novel component of the secretory pathway specifically required for localization of amino acid permeases in yeast. Cell 71, 463–478.

López-Otín C, Bond JS (2008). Proteases: multifunctional enzymes in life and disease. J Biol Chem 283, 30433–30437.

Manford AG, Stefan CJ, Yuan HL, MacGurn JA, Emr SD (2012). ER-to-plasma membrane tethering proteins regulate cell signaling and ER morphology. Dev Cell 23, 1129–1140.

Martins A, Pfirrmann T, Heessen S, Sundqvist G, Bulone V, Andréasson C, Ljungdahl PO (2018). Ssy5 is a signaling serine protease that exhibits atypical biogenesis and marked S1 specificity. J Biol Chem 293, 8362–8378.

Omnus DJ, Ljungdahl PO (2013). Rts1-protein phosphatase 2A antagonizes Ptr3-mediated activation of the signaling protease Ssy5 by casein kinase I. Mol Biol Cell 24, 1480–1492.
Omnus DJ, Ljungdahl PO (2014). Latency of transcription factor Stp1 depends on a modular regulatory motif that functions as cytoplasmic retention determinant and nuclear degron. Mol Biol Cell 25, 3823–3833.
Omnus DJ, Manford AG, Bader JM, Emr SD, Stefan CJ, Spang A (2016). Phosphoinositide kinase signaling controls ER-PM cross-talk. Mol Biol Cell 27, 1170–1180.
Omnus DJ, Pfirrmann T, Andréasson C, Ljungdahl PO (2011). A phosphodegron controls nutrient-induced proteasomal activation of the signaling protease Ssy5. Mol Biol Cell 22, 2754–2765.
Pfirrmann T, Heessen S, Omnus DJ, Andréasson C, Ljungdahl PO (2010). The prodomain of Ssy5 protease controls receptor-activated proteolysis of transcription factor Stp1. Mol Cell Biol 30, 3299–3309.
Poulsen P, Lo Leggio L, Kielland-Brandt MC (2006). Mapping of an internal protease cleavage site in the Ssy5p component of the amino acid sensor of *Saccharomyces cerevisiae* and functional characterization of the resulting pro- and protease domains by gain-of-function genetics. Eukaryot Cell 5, 601–608.
Rhee Y, Gurel F, Gafni Y, Dingwall C, Citovsky V (2000). A genetic system for detection of protein nuclear import and export. Nat Biotechnol 18, 433.
Robinson JS, Klionsky DJ, Banta LM, Emr SD (1988). Protein sorting in *Saccharomyces cerevisiae*: isolation of mutants defective in the delivery and processing of multiple vacuolar hydrolases. Mol Cell Biol 8, 4936–4948.
Silve S, Volland C, Garnier C, Jund R, Chevallier MR, Haguenauer-Tsapis R (1991). Membrane insertion of uracil permease, a polytopic yeast plasma membrane protein. Mol Cell Biol 11, 1114–1124.
Stefan CJ, Manford AG, Emr SD (2013). ER–PM connections: sites of information transfer and inter-organelle communication. Curr Opin Cell Biol 25, 434–442.
Stöven S, Silverman N, Junell A, Hedengren-Olcott M, Erturk D, Engström Y, Maniatis T, Hultmark D (2003). Caspase-mediated processing of the *Drosophila* NF-κB factor Relish. Proc Natl Acad Sci USA 100, 5991–5996.
Tumusiime S, Zhang C, Overstreet MS, Liu Z (2011). Differential regulation of transcription factors Stp1 and Stp2 in the Ssy1-Ptr3-Ssy5 amino acid sensing pathway. J Biol Chem 286, 4620–4631.
Turk B (2006). Targeting proteases: successes, failures and future prospects. Nat Rev Drug Discov 5, 785–799.
Turk B, Turk D, Turk V (2012). Protease signalling: the cutting edge. EMBO J 31, 1630–1643.
Wielemans K, Jean C, Vissers S, André B (2010). Amino acid signaling in yeast: post-genome duplication divergence of the Stp1 and Stp2 transcription factors. J Biol Chem 285, 855–865.
Wu B, Ottow K, Poulsen P, Gaber RF, Albers E, Kielland-Brandt MC (2006). Competitive intra- and extracellular nutrient sensing by the transporter homologue Ssy1p. J Cell Biol 173, 327–331.